

1           **Au Single Atoms Anchored WO<sub>3</sub>/TiO<sub>2</sub> Nanotubes for Photocatalytic**  
2                           **Degradation of Volatile Organic Compounds**

3           Xiaoguang Wang<sup>a</sup>, Honghui Pan<sup>a</sup>, Minghui Sun<sup>a</sup>, Yanrong Zhang<sup>a\*</sup>

4    <sup>a</sup>*School of Environmental Science and Engineering, Huazhong University of Science*  
5                           *and Technology, Wuhan, 430074, P.R. China*

7                           \*Corresponding author information:

8                           *Prof. Yanrong Zhang*

9                           *E-mail: yanrong\_zhang@hust.edu.cn*

10                          *Phone: +86 27 87793001; Fax: +86 27 87793001*

11

12

13

14

15

16

17

18

19

20

21

22

23

24

25

26

27

28

29

30

31

## 32 **TiO<sub>2</sub> nanotubes preparation and WO<sub>3</sub> loading**

33 The self-organized TiO<sub>2</sub> nanotubes (TNTs) were first prepared through our  
34 previously developed electrochemical anodization. Briefly, A two electrode  
35 electrochemical system was used for the anodization process employing a pieces of 1  
36 cm×3 cm of Ti foil and platinum mesh electrodes as anode and cathode respectively  
37 at a constant potential of 60 V for a period of 8 h with the 100 ml electrolyte  
38 containing 0.25 wt% NH<sub>4</sub>F, 13.7 vol% water and 86.3 vol% Ethylene glycol after a  
39 chemical polishing treatment with a solution containing HF, HNO<sub>3</sub> and H<sub>2</sub>O. Then,  
40 the resulting Ti foil was annealed in air at 450 °C for 2 h to obtain anatase TNTs. The  
41 loading of WO<sub>3</sub> on TNTs was accomplished by electrochemical deposition. In a three-  
42 electrode system, the above TNTs used as working electrode was immersed in a 100  
43 ml mixed solution containing Na<sub>2</sub>WO<sub>4</sub>, CH<sub>3</sub>COONH<sub>4</sub> and EDTA at a concentration  
44 of 0.1M with the immersion area of 1 cm×2 cm, then, was deposited  
45 electrochemically with WO<sub>3</sub> precursor under a constant current conditions of -4 mA (-  
46 2 mA/cm<sup>2</sup>) for a period of 10 min. The platinum electrode and the saturated calomel  
47 electrode (SCE) were counter electrode and reference electrode, respectively. After  
48 the electrochemical deposition, the as-prepared samples was cleaned with deionized  
49 water, dried at 60 °C and annealed in ambient atmosphere at 450 °C for 2 h with a  
50 heating rate of 5 °C/min. The distance between the electrodes was fixed at 3 cm in all  
51 the experiments.

52

## 53 **Photocatalyst Characterization.**

54 The properties of samples were analyzed by following spectroscopic analysis: field  
55 emission scanning electron microscope (FE-SEM, NANOSEM 450, FEI) and a field  
56 emission transmission electron microscope (TEM, Tecnai G2 F30, FEI) operating at  
57 an accelerating voltage of 30 kV, the elemental distribution was visualized by energy  
58 dispersive spectroscopy (EDS) of Oxford Instruments, X-ray diffraction (XRD,  
59 Rigaku Corporation, Japan) equipped with Cu-K radiation (40 kV, =1.5406 Å),

60 diffuse reflectance UV–visible absorption spectroscopy (DRS, UV-2550, Japan). X-  
61 ray photoelectron spectroscopy with an Axis Ultra instrument (XPS, Kratos  
62 Analytical), photoluminescence emission spectroscopy (PL, FP-6500, Jasco), in situ  
63 FTIR spectrometer equipped with photocatalytic reaction cell (Vertex 70v, Bruker),  
64 electron paramagnetic resonance spectroscopy (EPR, EMXnano, Bruker), the solid  
65 powder applied to OVs was scraped from the flaky sample with a cleaning knife.

66 Hard XAFS measurement was recorded at the XAS station (BL11) of the Saga  
67 Synchrotron Light Research Center, Japan. The hard X-ray was monochromatized  
68 with Si (111) double-crystals. W L<sub>3</sub>-edge and Ti K-edge XANES was recorded in a  
69 transmission mode.

70

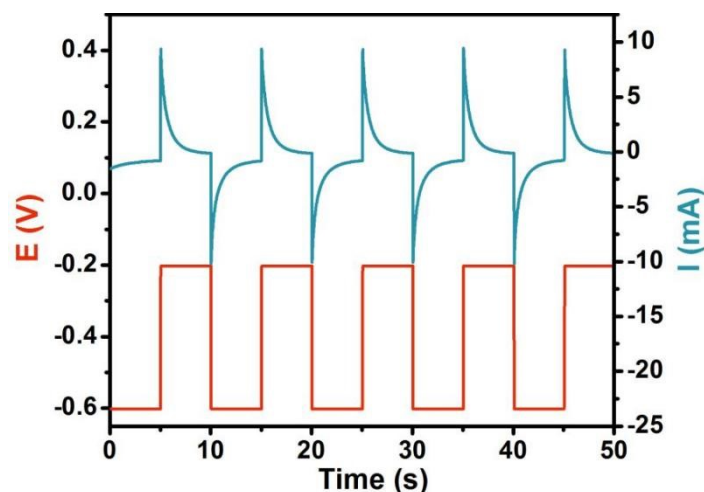
#### 71 IPCE

72 The irradiation intensity was measured by using a spectroradiometer (PL-MW2000,  
73 China). The average irradiation intensity of a 365 nm LED. The incident photon to  
74 current conversion efficiency (IPCE) and the apparent quantum yield (AQY) was  
75 calculated by using the following equation:<sup>21</sup>

$$76 \quad \text{IPCE (\%)} = 1240 \frac{I_p(\lambda)}{P_{inc}(\lambda) \lambda} \times 100 \quad (1)$$

77 where  $I_p(\lambda)$  is the photocurrent density (A m<sup>-2</sup>) at 1.0 V bias and  $P_{inc}(\lambda)$  is the  
78 incident power density of light (W m<sup>-2</sup>) at average wavelength  $\lambda$  (nm).

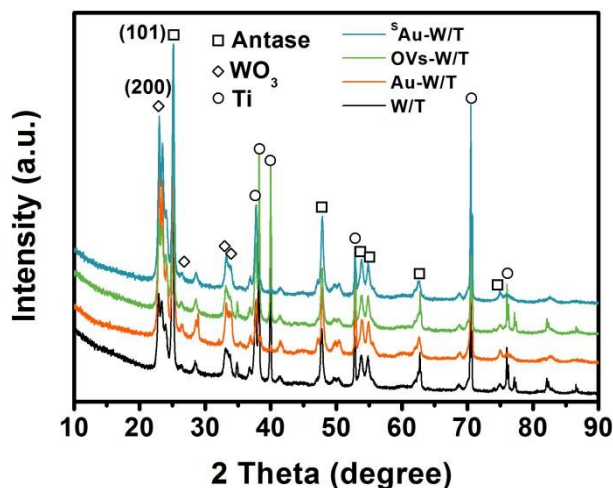
79



80

81 **Fig. S1**  $I$ - $V$  curves of square wave pulse method for anchoring Au atoms on OVs-  
 82  $\text{WO}_3/\text{TNTs}$

83



84

85 **Fig. S2** XRD spectra of W/T, Au-W/T, OVs-W/T and  $^s\text{Au}$ -W/T. For both W/T,  $^s\text{Au}$ -  
 86 W/T and  $^s\text{Au}$ -T/W composites, besides characteristic diffraction peaks of anatase  
 87  $\text{TiO}_2$  (JCPDF no. 21-1272), a couple of alternative peaks observed at  $24.4^\circ$  and  $26.6^\circ$   
 88 indicated the (200) and (101) planes of monoclinic  $\text{WO}_3$  (JCPDS no. 97-001-4332),  
 89 respectively.

90

91 **Table S1** The specific surface area ( $S_{\text{BET}}$ ) and Au content of samples. The  $\text{N}_2$   
 92 adsorption/desorption measurements were performed on the samples with peeling off  
 93 the powder from the Ti substrate. Au content was measured by ICP-AES.

samples	$S_{\text{BET}}$ ( $\text{m}^2/\text{g}$ )	Au content (wt %)
$^s\text{Au}$ -T/W	0.343	2.41
OVs-W/T	0.339	—
Au-W/T	0.327	3.28
W/T	0.327	—

94

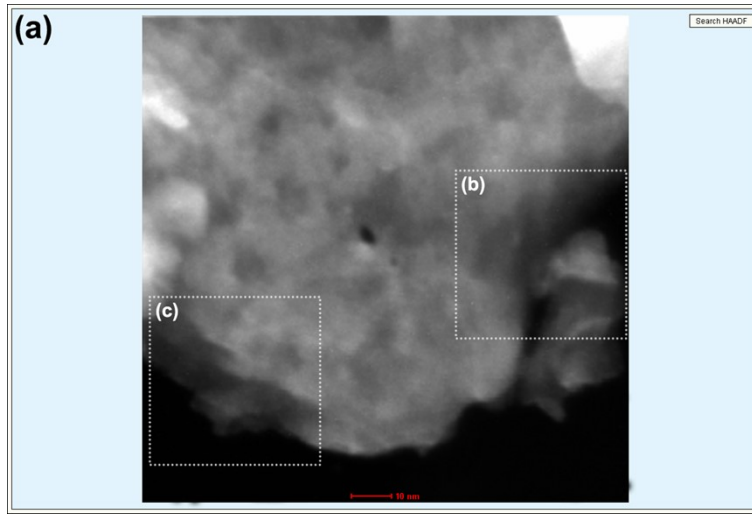
95

96

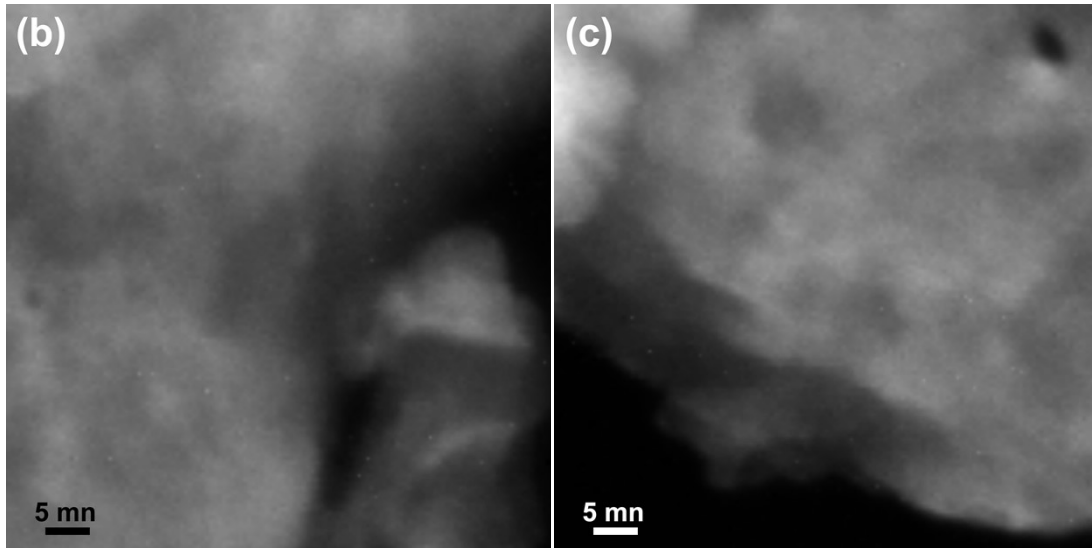
97

98

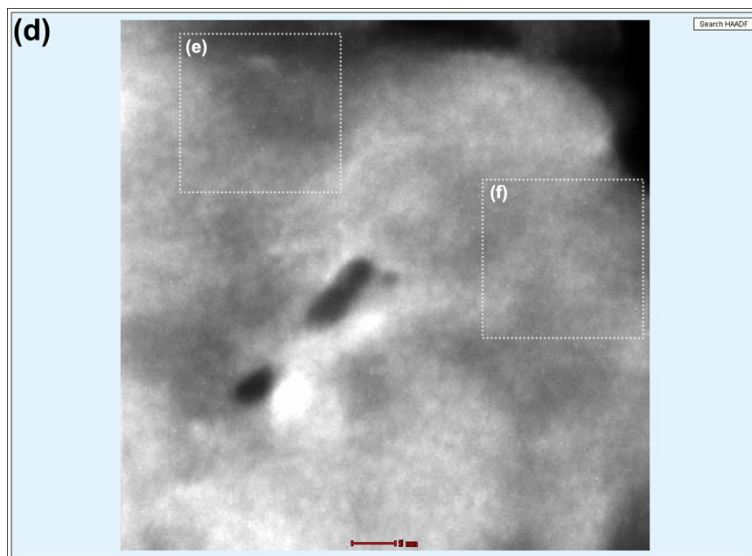
99



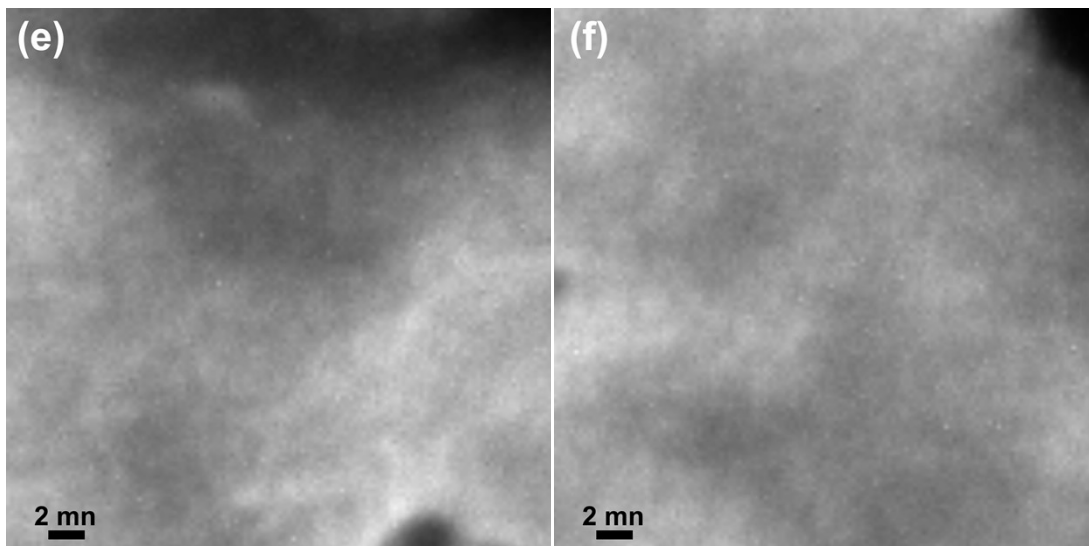
100



101



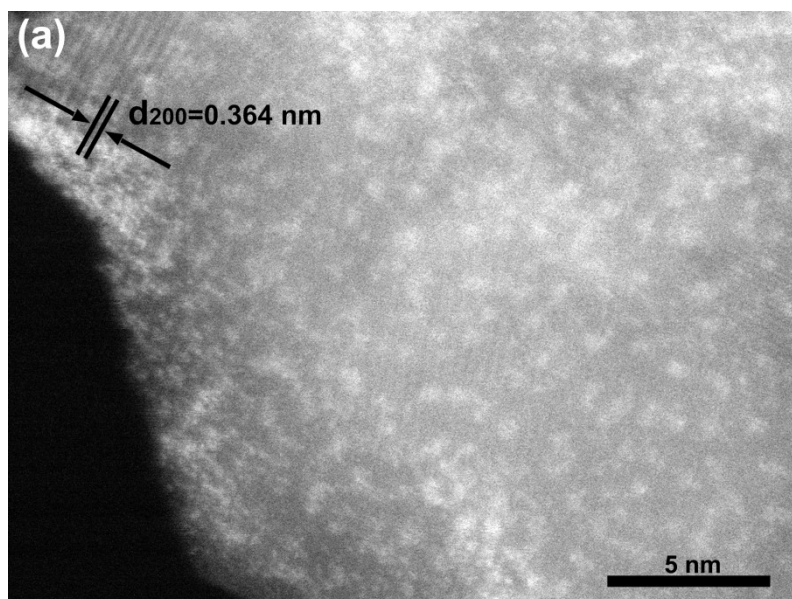
102



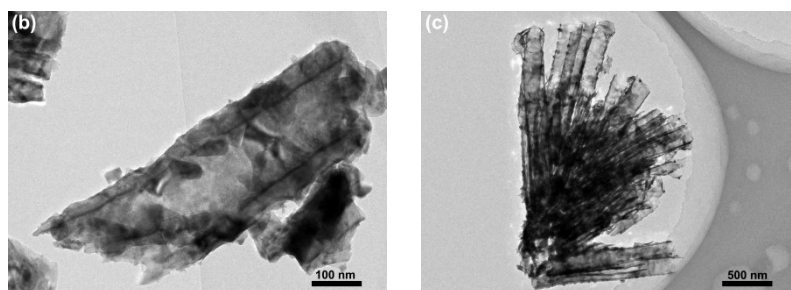
103

104 **Fig. S3** (a) HAADF-STEM images of  $^S\text{Au-W/T}$ . A large number of bright spots could  
 105 be observed on the surface of the support.

106



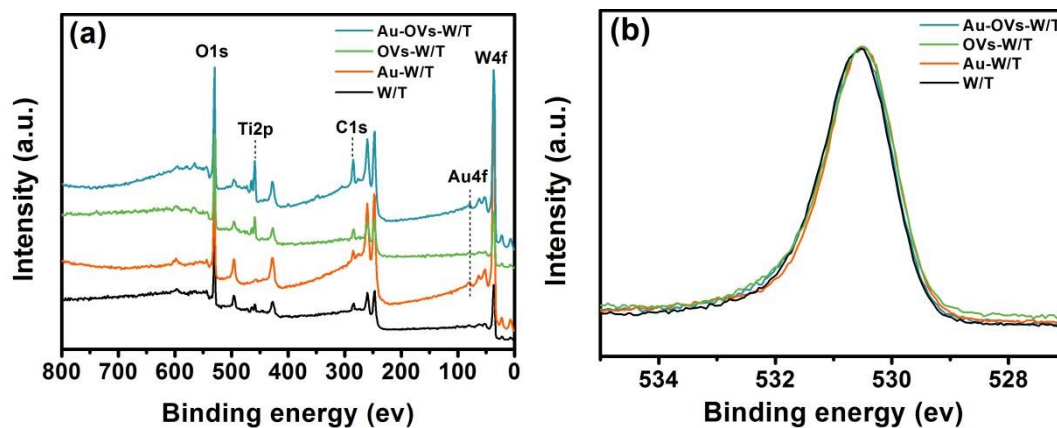
107



108

109 **Fig. S4** (a) HAADF-STEM image and (b) (c) STEM image of Au-W/T. Au was  
 110 dispersed on the surface of  $\text{WO}_3$  as cluster consisting of several Au atoms.

111



112

113 **Fig. S5** (a) XRD spectra and (b) O1s XPS spectra of samples.

114

115 **Table S2.** BE and PA of W 4f, and MP of W<sup>5+</sup> and W<sup>6+</sup> species of samples

Samples	BE (eV)				PA (Counts)				MP (%)	
	W <sup>6+</sup>		W <sup>5+</sup>		W <sup>6+</sup>		W <sup>5+</sup>		W <sup>6+</sup>	W <sup>5+</sup>
	4f <sub>5/2</sub>	4f <sub>7/2</sub>	4f <sub>5/2</sub>	4f <sub>7/2</sub>	4f <sub>5/2</sub>	4f <sub>7/2</sub>	4f <sub>5/2</sub>	4f <sub>7/2</sub>		
<sup>s</sup> Au-T/W	37.59	35.52	37.02	34.98	32186.0	34285.3	6127.7	10375.1	80.1	19.9
OVs-W/T	37.59	35.51	37.04	34.98	25370.2	27782.0	11086.2	18796.5	64.0	36.0
Au-W/T	37.62	35.53	37.02	34.97	12695.6	13992.7	1063.9	2602.5	87.9	12.1
W/T	37.61	35.54	37.01	34.98	43842.1	48758.9	5009.1	7258.6	88.3	11.7

116

117 **Table S3** Binding energy (BE) and relative peak area (PA) of Ti 2p, and molar  
118 percentages (MP) of samples

Samples	BE (eV)				PA (Counts)				MP (%)	
	Ti <sup>4+</sup>		Ti <sup>3+</sup>		Ti <sup>4+</sup>		Ti <sup>3+</sup>		Ti <sup>4+</sup>	Ti <sup>3+</sup>
	2p <sub>1/2</sub>	2p <sub>3/2</sub>	2p <sub>1/2</sub>	2p <sub>3/2</sub>	2p <sub>1/2</sub>	2p <sub>3/2</sub>	2p <sub>1/2</sub>	2p <sub>3/2</sub>		
<sup>s</sup> Au-T/W	464.99	459.17	464.09	458.73	5807.8	12983.7	1570.5	1065.6	87.7	15.3
OVs-W/T	465.00	459.18	464.11	458.72	2738.4	8126.2	1224.2	952.8	83.3	16.7
Au-W/T	465.00	459.15	464.12	458.73	2893.4	6213.7	282.2	495.7	92.1	7.9
W/T	465.00	459.18	464.10	458.75	8611.8	15126.9	689.9	1148.5	92.8	7.2

119

120 **Table S4** IPCE and the AQY of R-WO<sub>3</sub>/TNTs and WO<sub>3</sub>/TNTs

Samples	W/T	Au-W/T	OVs-W/T	<sup>s</sup> Au-W/T
Illuminant	365 nm LED			
Average wavelength (nm)	365 nm	365 nm	365 nm	365 nm
Power density (W cm <sup>-2</sup> )	0.132	0.132	0.132	0.132
Photocurrent (mA cm <sup>-2</sup> )	0.11	0.82	1.14	1.79
IPCE (%)	0.70	5.19	7.22	11.34

121

122 **Table S5** IR modes assigned to various functional groups identified in the in-situ

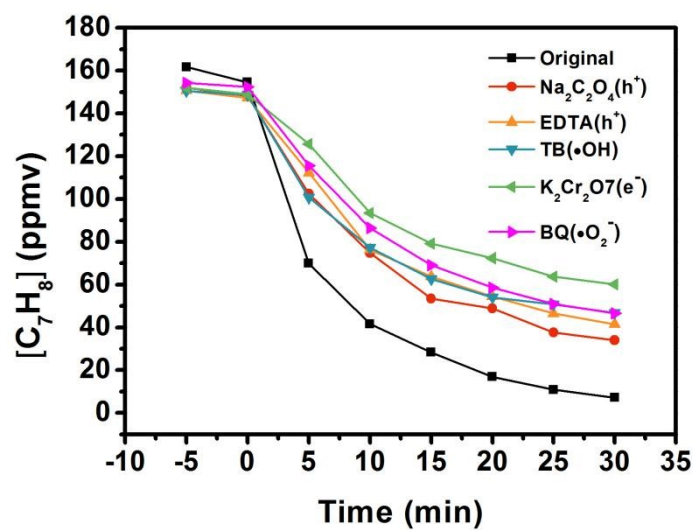
123 FTIR photodegradation spectra of toluene.

IR modes	Functional group
1610 cm <sup>-1</sup> 1500 cm <sup>-1</sup> 1599 cm <sup>-1</sup> 1492 cm <sup>-1</sup>	skeleton stretching and bending vibrations of aromatic ring
2361 cm <sup>-1</sup> 2340 cm <sup>-1</sup>	C=O stretching vibrations of CO <sub>2</sub>
1467 cm <sup>-1</sup> 1462 cm <sup>-1</sup>	C-O stretching vibration of benzyl alcohol
1690 cm <sup>-1</sup> 1676 cm <sup>-1</sup>	stretching vibration of aldehydes
1565 cm <sup>-1</sup> 1548 cm <sup>-1</sup> 1529 cm <sup>-1</sup>	asymmetric stretching vibration of the carboxylate group COO <sup>-</sup> from benzoic acid
1581 cm <sup>-1</sup> 1481 cm <sup>-1</sup>	the C=C stretching vibration of benzoic acid
1658 cm <sup>-1</sup>	p-benzoquinone-type species
1510 cm <sup>-1</sup>	C = O stretching vibrations of maleate
1413 cm <sup>-1</sup>	C = O stretching vibrations of saturated aliphatic acids (formate and acetate)
1442 cm <sup>-1</sup>	COO <sup>-</sup> stretching vibration of the maleate species
1640 cm <sup>-1</sup> 1630 cm <sup>-1</sup>	surface water species
2884 cm <sup>-1</sup> 2937 cm <sup>-1</sup>	C-O stretching vibration mode of aromatic ring
3695 cm <sup>-1</sup> 3682 cm <sup>-1</sup>	bridged-OH acted as the adsorption sites



3662 cm <sup>-1</sup>	
3641 cm <sup>-1</sup>	
3603 cm <sup>-1</sup>	
3621 cm <sup>-1</sup>	O-H bending and stretching vibrations of carboxylic acids
3739 cm <sup>-1</sup>	
3727 cm <sup>-1</sup>	
3716 cm <sup>-1</sup>	O-H stretching vibration of the terminal hydroxyls, •OH radicals
3704 cm <sup>-1</sup>	

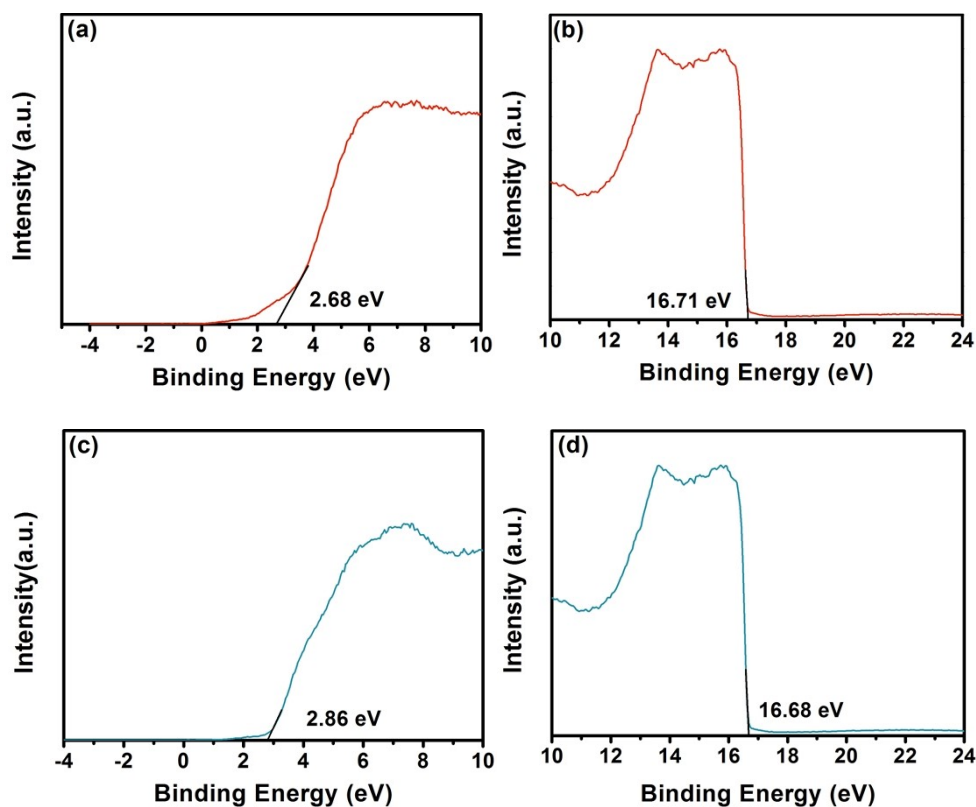
124



125

126 **Fig. S6** Quenching experiment over <sup>S</sup>Au-W/T. the quenchers were loaded on surface  
 127 of <sup>S</sup>Au-W/T film by impregnation method. In detail, the film was impregnated into a  
 128 quencher solution with a 0.1 mM concentration for 30 min followed by a drying at 60  
 129 °C, then was used for degradation of toluene.

130



131

132

133 **Fig. S7** UPS measurements for electrochemically reduced (a, b) TiO<sub>2</sub> and (c, d) WO<sub>3</sub>.

134 The work function ( $\phi$ ) of TiO<sub>2</sub> was calculated to be 4.44 eV ( $h\nu - W = 21.22$  eV -  
 135 16.71 eV = 4.51 eV). Its band gap between Fermi level ( $E_f$ ) and the VB maxima (VBM)  
 136 was 2.68 eV. Therefore, TiO<sub>2</sub> catalyst turned out to have VBMs ( $E_{VBM} + E_\phi - 4.5$  V)  
 137 and CB ( $E_g - E_{VBM}$ ) at 2.61 and -0.56 V vs. NHE, respectively. Likewise, WO<sub>3</sub> was  
 138 turned out to have VBMs and CB at 2.90 and 0.12 V vs. NHE, respectively. UPS  
 139 curve of the electrochemically reduced WO<sub>3</sub> was obtained by measuring the WO<sub>3</sub>  
 140 loaded on a Ti foil.

141

142